Nuclear Materials and Energy 12 (2017) 1324–1329

Contents lists available at ScienceDirect

Nuclear Materials and Energy

journal homepage: www.elsevier.com/locate/nme

Flowing liquid lithium plasma-facing components – Physics, technology and system analysis of the LiMIT system

D.N. Ruzic[a], M. Szott[a,*], C. Sandoval[b], M. Christenson[a], P. Fiflis[a], S. Hammouti[a], K. Kalathiparambil[a], I. Shchelkanov[a], D. Andruczyk[a], R. Stubbers[c], C. Joel Foster[c], B. Jurczyk[c]

[a] Department of Nuclear, Plasma and Radiological Engineering, University of Illinois, Urbana, IL 61801, USA
[b] CICATA Querétaro, Cerro Blanco 141, Col. Colinas del Cimatario, Querétaro, QRO, C.P. 76090 Mexico
[c] Starfire Industries, LLC, Champaign, IL 61820

ARTICLE INFO

Article history:
Received 15 July 2016
Revised 26 May 2017
Accepted 1 June 2017
Available online 29 July 2017

Keywords:
Liquid lithium
Plasma-facing components
Thermoelectric magnetohydrodynamics

ABSTRACT

The use of low atomic number liquid metals has been shown to have the potential to solve many of the prevalent problems like erosion and radiation losses associated with the interaction of fusion plasma with the plasma facing component (PFC) structures in tokamaks. Since the first evidence of lithium increasing plasma performance in TFTR [1], the benefits of using lithium in fusion environments have been seen in many devices, including CDX-U [2], NSTX [3], LTX [4], and DIII-D [5]. While both fast flow and slow flow concepts have been studied with regards to liquid lithium first wall alternatives, this report will focus on efforts placed on fast flow research and will mainly focus on advancements in the LiMIT device that help to eliminate concerns over the broad use of liquid lithium. Due to the promising TFTR results along with results obtained at the University of Illinois at Urbana-Champaign [6], suitably designed trench structures holding liquid lithium could be an appropriate fast flow candidate for PFC modules in future fusion devices. There are four potential shortcomings of this approach: (1) Droplet ejection, (2) Wetting control, (3) Tritium retention, and (4) Limited heat flux handling. Droplet ejection is discussed in a companion publication [7], while this paper addresses the topics of wetting control and heat flux handling. Limitations in wetting and prevention of lithium creep (i.e. getting and keeping the lithium only where it should be) have been solved by laser-texturing the base material with extreme short laser pulses (pico – femto second) of high power (several 10 s of W). Micro- and nano-structuring results indicate that the textured substrates displayed significant change in their wetting properties, increasing the temperature needed to wet from 310 °C to 390 °C. Lastly, initial designs for the Lithium Metal Infused Trenches (LiMIT) [6] showed dryout above 3 MW/m^2, but new designs of the trench shaping show potential to be able to handle up to 10 MW/m^2. Dryout is accompanied by lithium evaporation which is shown to mitigate the incident heat flux, which may be viewed as beneficial [8]. The advances shown here will increase the viability of the LiMIT system in large-scale testing, and allow for extensive design iteration to begin tackling the large powers and heat fluxes present in reactor-relevant systems.

1. Introduction

One of the primary issues fusion energy faces is the material choice for plasma confinement. Even solid refractory metal wall materials have exhibited issues that could eventually lead to confinement failure [9] or tritium inventory problems [10]. Liquid lithium can offer a number of advantages over solid materials at these interfaces, but is not without its own issues. This paper will describe progress in addressing a few of the concerns surrounding wetting control and heat flux handling with respect to the LiMIT system [6].

Liquid metals suffer from technological limitations associated with the need to continuously heat the metal to keep it in its liquid form, while wetting dissimilar metal surfaces. While the wetting temperature can be controlled through different pre-treatment means [11], there are many areas in a fusion device where liquid metal contact is unwanted. This report presents results showing

* Corresponding author.
E-mail addresses: druzic@illinois.edu (D.N. Ruzic), szott1@illinois.edu (M. Szott).

http://dx.doi.org/10.1016/j.nme.2017.06.001

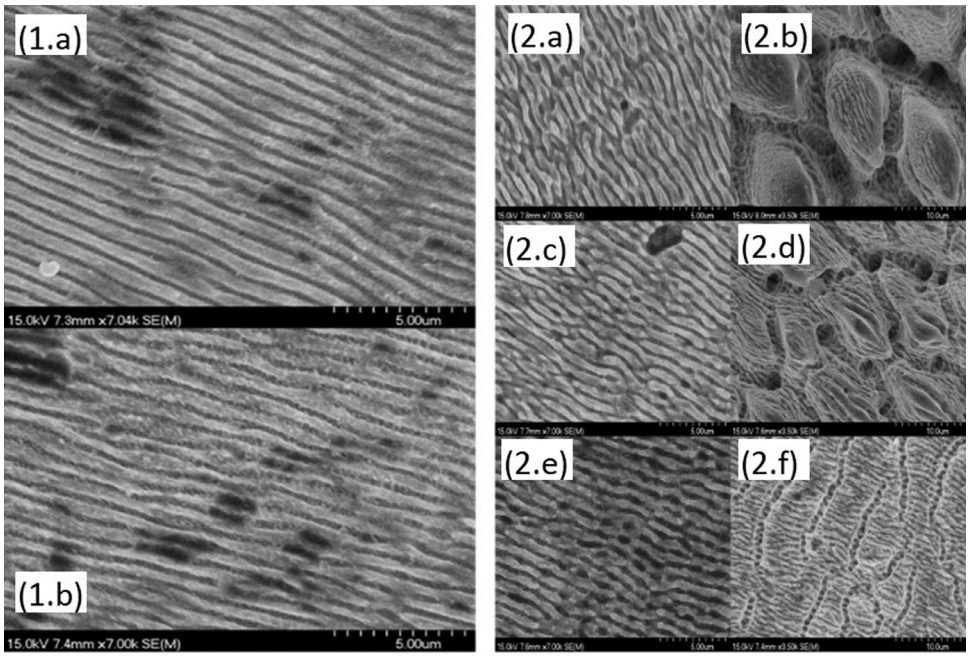

Fig. 3.1. Scanning electron microscopy images of the molybdenum samples (1.a, 1.b) and the 316 stainless steel samples (2.a – 2.f). The lithium contact angle studies were performed on the samples 1.a and 2.b. Molybdenum samples show a change in surface morphology under various laser power densities, while steel samples show changes based on the number of passes the laser made over a single radial position.

that making micro- and nano-textured surfaces can prevent unwanted liquid metal wetting in areas by increasing the temperature needed to uniformly wet the surface.

As plasma flux impinges on the LiMIT system, the lithium is locally accelerated where the plasma flux is greatest, due to the higher heat load creating a stronger thermoelectric driving force. This causes a depression of the lithium surface and pileup of the lithium downstream of the plasma flux. If the depression is too pronounced, the tops of the trench system may become exposed, leading to the problem called lithium dryout. If dryout occurs in fusion relevant conditions, the plasma striking the solid surface could damage the LiMIT module and sputter impurities into the plasma edge. This effect was observed at high heat loads in Illinois [7] and in Magnum PSI [12], and must be addressed if LiMIT is to be applied to large-scale systems.

2. Materials and methods

2.1. Nanostructuring and wetting

To generate nanostructured surfaces on various 316 stainless steel and molybdenum circular targets, the samples were processed with an IMRA North America 10 W, 350 fs near-infrared (1045 nm) fiber laser at a 1 MHz repetition rate. With a focal spot size between 10–30 µm, the samples were mounted on a rotational stage integrated to an x-stage scanner to allow high-speed laser scanning while moving the x-stage radially outward or inward. This was done in an effort to increase the processing speed and access the transitional sub-ablation regime where non-linear laser effects modify the surface morphology [13]. To create both micro- and nano-features, the beam was slightly defocused to a 100 µm beam spot. The primary features formed ranged in thickness from 0.5 to 1 µm. The surface structure topology was quantified using a Sloan Dektak^3 profilometer at the University of Illinois Frederick Seitz Materials Research Laboratory. Scanning electron microscopy images of the surfaces subjected to a variety of laser conditions were taken on a Hitachi S4700 High Resolution SEM at the University of Illinois Frederick Seitz Materials Research Laboratory. Visual inspection revealed optical fringing patterns and iridescence from a combination of geometric patterns and surface oxide layers.

Investigations of the contact angle of lithium on nanostructured surfaces were carried out in the setup used in Fiflis, et al. [11]. The circular samples were placed on a stainless steel actuated plate in a vacuum chamber able to achieve a base pressure of 1×10^{-6} Torr. An injector was used to deposit controlled amounts of lithium onto the surface of these samples at different radial positions. A heater below the steel plate was used to control the temperature on the samples and a thermocouple monitored the change in surface temperature, while a camera took photographs of the droplets as a function of the surface temperature. A MATLAB program was then used to monitor the evolution of the contact angle from these photographs, with the critical wetting angle defined at 90°.

2.2. Dryout and heat flux handling

In order to work towards mitigating dryout, a 2-dimensional free-surface lithium flow model was developed in COMSOL Multiphysics to examine the dryout phenomenon. The model utilizes the Laminar Flow and Moving Mesh modules. A Gaussian heat flux input on the top surface mimics the plasma heat flux, and cooling on the bottom of the domain provides the thermal gradient required to drive the thermoelectric magnetohydrodynamic (TEMHD) flow through the trench. This TEMHD force is included as a volume force, and the top surface of the domain is allowed to deform in response to the volume force in the x and y directions. The left and right surfaces act as a lithium flow inlet and outlet, respectively. This model utilizes the Arbitrary Lagrangian Eulerian method to power the mesh deformation, which couples the mesh movement with the fluid flow along the top surface.

3. Results

3.1. Nanostructuring and wetting

A peculiarity of the ultra-short laser-matter interaction is the formation, under specific conditions, of nano/micro (sometimes

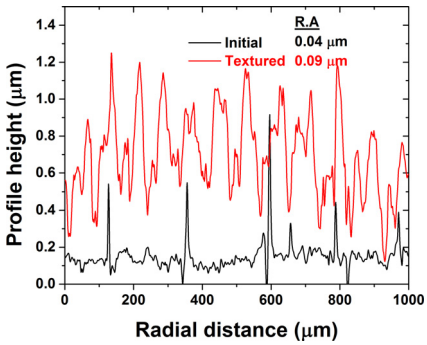

Fig. 3.2. Surface roughness of a stainless steel sample before and after laser texturing as measured through profilometry. The average surface roughness increases with laser exposure at all radial points.

multi-scale) periodic surface morphologies. One of the most remarkable phenomenon is the formation of periodic undulations called ripples or LIPSS [14]. In this study, ripples (described in Section 2.1) were systematically obtained at low power (5 W) and high scan velocity (1 MHz), for both materials. Fig. 3.1 shows SEM images of features observed after laser irradiation. The surface topography formation strongly depends on the laser fluence (J/cm^2) and the number of successive passes. Interestingly, in the case of stainless steel, the increase in successive passes (shown in the evolution of surface morphologies in Fig. 3.1) leads to the change from ripples to multi-scale columnar structures.

Profilometry measurements of the individual sample surfaces showed depth profiles of the micro- and nano-features when comparing before and after nano-texturing. This helped to quantify how laser texturing modified an individual surface. An example plot can be seen in Fig. 3.2. While the most prominent features are micro-scale, nano-scale structures can also be seen to have formed on these micro-features.

Fig. 3.3 shows a drastic increase in the temperature required to wet the laser textured samples when compared to bare samples of the same material [11]. The nanostructured molybdenum samples showed a 77 °C increase in the wetting temperature, while the steel samples showed an 83 °C increase. This increase in wetting temperature on the textured surfaces can be attributed to surface tension forces that prevent wetting in the surface features, as described by Cassie–Baxter theory [15], in combination with surface oxidation, which has shown to inhibit wetting [16]. To wet the surface, the droplet must transition through the Wenzel state [17] to a fully wetted front before macroscopic wetting can be observed. These results are crucial to the design process for lithiated assemblies because they indicate that wetting and flow of lithium can be controlled by modifying surface roughness. Fig. 3.1(1a) and 3.1(2b) shows SEM photos of the structured stainless steel and molybdenum samples obtained for one specific laser power and scanning speed. Those specific samples were used to obtain the wetting results in Fig. 3.3. The assembled laser set-up was used to process several other sets of substrates (results not presented in this work) by varying only power, laser focus, or sample translation/rotation speed.

3.2. Dryout and heat flux handling

While computational constraints made running a 2-dimensional simulation most viable for the free surface, moving mesh scenario, a 3-dimensional model of a LiMIT-style trench informed the initial conditions to boost model accuracy [18]. This 3-dimensional fixed surface model fully couples time varying electric currents and heat transfer in the solid and fluid domains to solve for the TEMHD driving force and associated circulating lithium flow. It included a Gaussian heat flux stripe with a peak of 3 MW/m^2 and a full width half maximum of 5 mm. This heat flux can be adjusted based on physical system parameters, but was chosen in this case to coincide with the electron beam tests of LiMIT at UIUC. A good example of the dryout seen in these tests is given in Fig. 3.4.

The velocity characteristics on the fixed surface of the 3D model imply a region in which dryout will form. Here, the centered external heat flux drives a high velocity region that gets pulled downstream by the flow circulation. The volume force profile is extracted and used as a 2-dimensional free surface model input. The 2-dimensional model assumes pre-circulating lithium flow, which can be experimentally maintained in the absence of a plasma heat flux by heating the back surfaces of the LiMIT system. As the simulation begins, the lithium surface starts to depress directly under the high heat flux stripe. This is due to the preferential heating of the lithium in the depressed region, which is then accelerated by the large thermal gradient resulting from passing through the heat stripe. The dryout depression is quickly propelled along the flow direction, as seen in Fig. 3.5A. Lithium buildup occurs on the downstream side due to flow accelerating into slower downstream flow, and can also be seen on the upstream side during the transient period of dryout development due to lithium building up against the reduced cross-sectional area before accelerating through the high heat flux region. This can be seen in Fig. 3.5B.

4. Discussion

The results in Section 3.1 are very promising for two reasons, both being caused by the surface roughening and the micro-scale and nano-scale patterning of the metal samples. Two theories are proposed for the observed increase in wetting temperature. First,

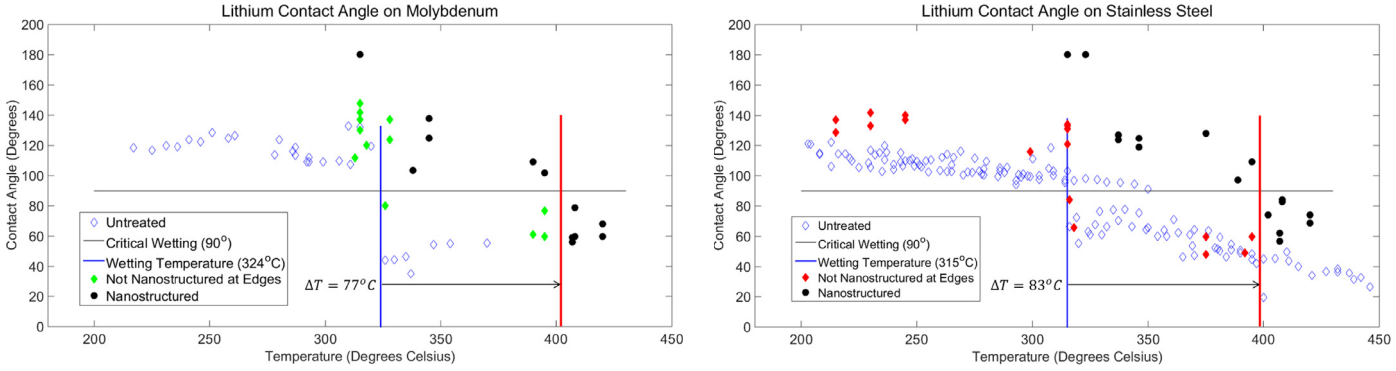

Fig. 3.3. The change in the wetting temperature for lithium on molybdenum (left) and stainless steel (right) surfaces. Wetting temperatures on the laser structured samples are compared to wetting temperatures on nominally smooth counterparts from this and previous work [11].

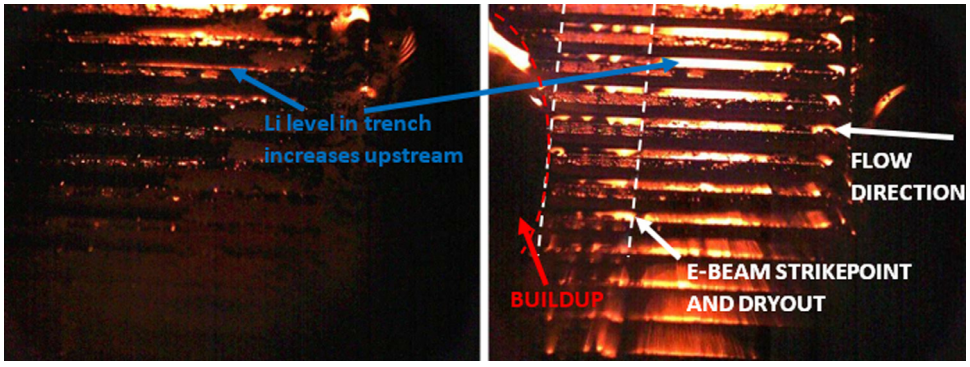

Fig. 3.4. Experimental observation of lithium dryout under electron beam impingement. Downstream lithium buildup is clearly seen, and, while the lithium level starts beneath the trench level, both lithium depression in the strike zone and upstream buildup are visible.

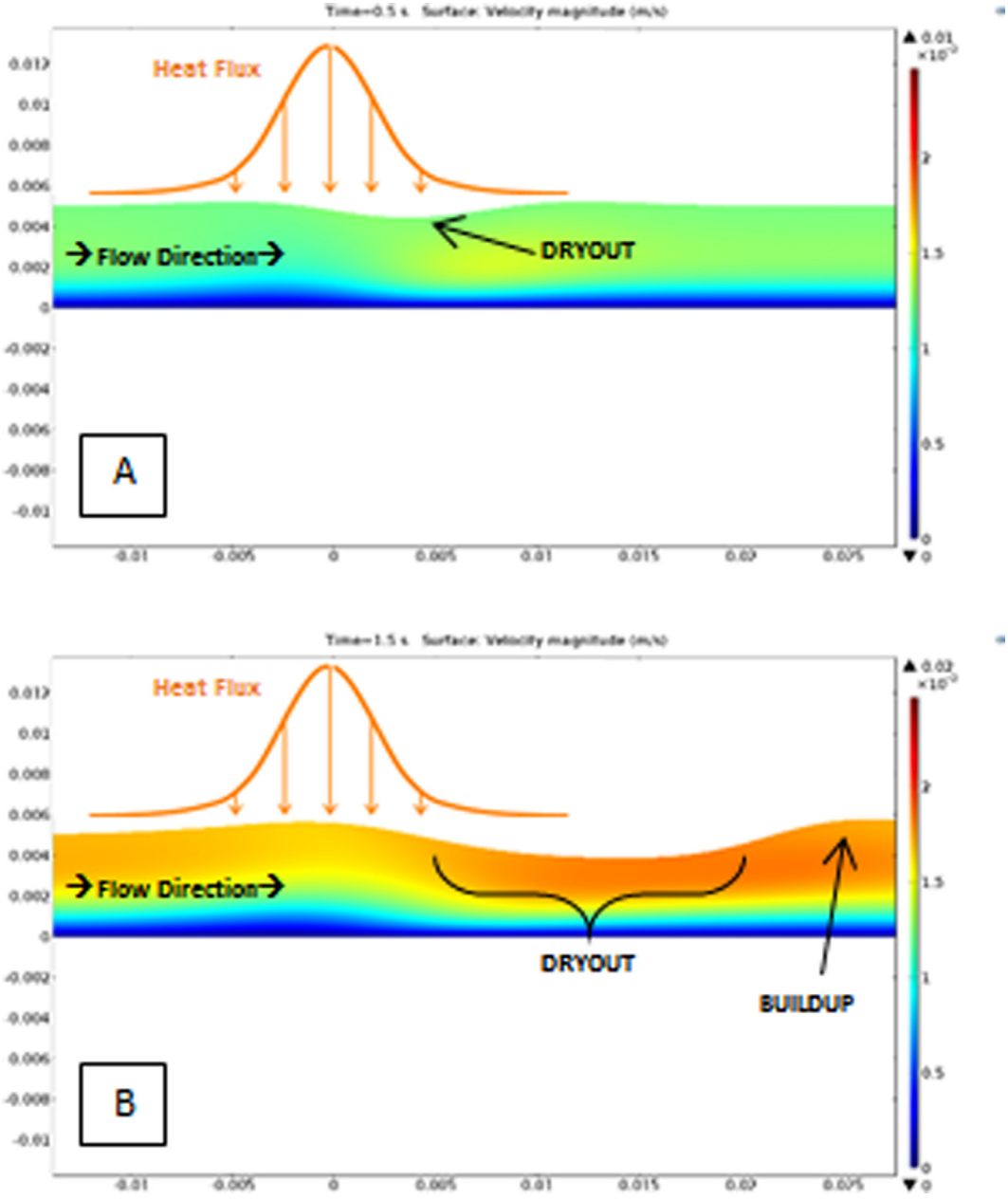

Fig. 3.5. A) The beginning of the lithium depression as dryout begins and is propelled downstream by lithium flow. B) Developed dryout phenomenon under high heat flux exhibits pronounced lithium depression and lithium buildup downstream. Distance is in meters and velocity values are in meters per second.

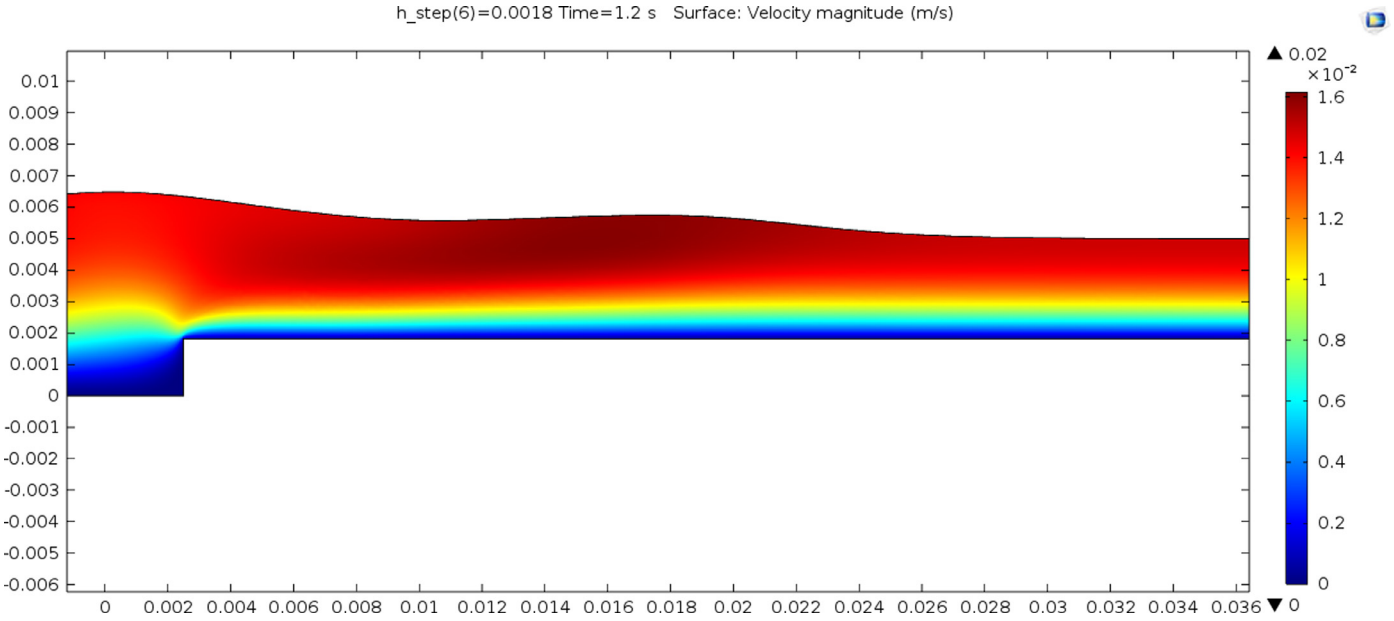

Fig. 4.1. The addition of a step increase in the height of the trench bottom works to mitigate dryout concerns. Upwelling at 0 m (highest heat flux) protects from further dryout, and the lithium level never falls below the 5 mm height of the trenches. Distance is in meters and velocity values are in meters per second.

the nanostructured surfaces form a larger, more robust oxide layer based purely on the increase in surface area when compared to their smooth counterparts. Lithium must first break through this oxide layer formed on the surface before propagating along the wetting front. Also, the nanostructured surfaces now contribute to increased surface tension forces between the three phases in contact - solid, liquid, and gas (in this case vacuum) - which inhibits wetting. The combined forces from the increased oxide layer and surface tension must be overcome before wetting can migrate through the transitions explained by the Cassie–Baxter [15] and Wenzel [17] theories. Based on a Cassie–Baxter theory analysis, the degree of wetting temperature increase can be related to a surface roughness coefficient known as the wetted area, which is a fractional area the surface structures occupy. As seen in Fig. 3.1, much of the surface morphology is similar to the trench-like structures of an ideal Cassie–Baxter wetting state. From experimental measurement of the fractional area of the structures, values of 0.73 and 0.68 were determined for molybdenum and stainless steel, respectively. The theoretical analysis yielded 0.75 and 0.70, showing that, to within measurement error, the increase in wetting temperature can be largely explained by changing surface morphology.

The reason these results are promising for larger scale devices is design-based. There exists an operating window in terms of temperature where one can safely flow liquid lithium without having significant evaporation from the surface. The wetting temperature on these nanostructured surfaces has been shown to be well outside this operating regime, meaning that design of such surfaces in a larger device will inhibit lithium wetting and creep in unwanted areas. LiMIT structures are envisioned to eventually cover the entirety of the limiter and divertor surfaces within a larger machine, if not the entire inner surface. One cannot make this a possibility without having small breaks between lithium-holding modules, similar to why the entirety of a divertor cannot be made out of one solid block of tungsten. The textured surfaces will act as a barrier in the chamfers and valleys between the LiMIT modules, which will be subjected to less heat and particle flux and will maintain temperatures below the wetting operating limits described in Section 3.2. These structured surfaces will act as creep barriers, protecting any sensitive systems set back from the first wall, like electronics or cooling lines needed to maintain the TEMHD flow. Overall, the results presented in this report lend more credence to the use of liquid lithium as a first wall material.

The simulation presented of the dryout phenomenon from Section 3.2 qualitatively mirrors experimental observations of LiMIT dryout at Illinois (see Fig. 3.4) and in devices such as Magnum PSI. This dynamic effectively captures how lithium dryout forms and progresses in high heat flux conditions; therefore, providing a valid basis for engineering decisions regarding a solution to the dryout effect. Potential mitigation strategies include trench shaping, partial trench removal, or a constraining mesh. Trench shaping would change the depth of the trenches in plasma-driven acceleration regions to compensate for the increased velocity. The partial trench removal avenue simply accounts for the existence of dryout by removing sections of the trench walls to account for plasma depression of the lithium surface and machining a larger outlet to avoid spillover from the buildup. A mesh can also be placed above the top surface of the trenches, which would stay wetted with liquid lithium and constrain the surface without impeding bulk lithium flow. Future trench designs or shaping inserts can be tested with this model before experimental application.

Several potential trench shaping mechanisms were investigated to attempt to alleviate the behavior seen in the model and inform future design. The most effective method turned out to be a step increase in the trench height placed slightly downstream from the highest heat flux point. The ledge creates an upwelling directly under the area of highest heat flux, helping to protect the trenches, while also minimizing the extent of dryout and therefore the downstream buildup height. This effect can be seen in Fig. 4.1, where an increase in trench height of 2.1 mm was used.

Further trench shaping can be studied for specific heat fluxes or trench designs based on the system in question, and the model results allow for rapid design iteration before building test modules. To prove viability of the LiMIT system in large scale devices like ITER, the system must be able to effectively handle heat loads of at least 10–20 MW/m^2 at magnetic fields up to 10 T, a conservative estimate based on ITER's maximum reported toroidal magnetic field. This is a significant jump from the 3 MW/m^2 and 0.1 T dryout simulations in this paper. At fusion relevant magnetic fields, B $>$ 1 T, TEMHD-driven lithium velocity is inversely related to magnetic field, namely $v \propto S\nabla T/B$ [18]. It is also important to recognize

the direct dependence on the thermal gradient. As the magnetic field increases, the thermal gradient must also increase in order to maintain similar flow velocities. Computational work done at UIUC has determined that a heat transfer coefficient of $> 4\,kW/m^2K$ is required to produce the temperature gradient necessary for effective LiMIT operation at fusion relevant magnetic fields [18]. While experimental tests at UIUC have only ever utilized compressed air cooling, water, helium, or liquid metal cooling can drastically increase heat transfer, and advanced concepts such as T-tube cooling could eventually be used to achieve heat transfer coefficients up to $40\,kW/m^2K$ [19]. Additionally, stationary liquid lithium has been shown to effectively dissipate beam spot power of up to $60\,MW/m^2$ in CDX-U with no local or bulk evaporation, due to a combination of MHD effects and the Marangoni effect [20]. Coupled with lithium flow, this ability will allow the LiMIT system to dissipate transient events of locally higher heat fluxes without fully disrupting the system flow and exhibiting destructive dryout. This is supported by early computational models of the LiMIT system [18], while experimentation is continuing to address the challenges of increasing performance to these metrics.

5. Conclusions

Liquid metals have shown great promise as plasma-facing components, having many advantages over solid materials. However, several technological challenges remain. This paper has addressed some of the issues under investigation, including control of liquid metals via surface texturing and early models of liquid metal dryout and potential mitigation techniques. While extensive design iteration and testing is necessary to implement liquid metal plasma-facing component concepts as full-scale reactor relevant devices, these advances enhance the LiMIT system to allow testing in modern large-scale devices.

Acknowledgment

This work was supported at Illinois by the Department of Energy, Office of Fusion Energy Sciences grants, DE-SC0008587, DE-SC0008658, and DE-FG02-99ER54515.

References

[1] J. Li, et al., A long-pulse high-confinement plasma regime in the Experimental Advanced Superconducting Tokamak, Nat. Phys. 9 (2013) 817–821.
[2] R. Majeski, et al., CDX-U operation with a large area liquid lithium limiter, J. Nucl. Mater. 313 (2003) 625–629.
[3] R. Maingi, et al., The effect of progressively increasing lithium coatings on plasma discharge characteristics, transport, edge profiles and ELM stability in the national spherical torus experiment, Nucl. Fus. 52 (8) (2012) 083001. https://doi.org/10.1088/0029-5515/52/8/083001.
[4] J.C. Schmitt, et al., High performance discharges in the Lithium Tokamak eXperiment with liquid lithium walls, Phys. Plasmas 22 (5) (2015) 056112. https://doi.org/10.1063/1.4921153.
[5] A. Bortolon, et al., High frequency pacing of edge localized modes by injection of lithium granules in DIII-D H-mode discharges, Nucl. Fus. 56 (5) (2016) 056008. https://doi.org/10.1088/0029-5515/56/5/056008.
[6] D.N. Ruzic, W. Xu, D. Andruczyk, M.A. Jaworski, Lithium-metal infused trenches (LiMIT) for heat removal in fusion devices, Nucl. Fus. 51 (2011) 102002.
[7] P. Fiflis, M. Christenson, M. Szott, K. Kalathiparambil, D.N. Ruzic, "Free surface stability of liquid metal plasma facing components", *Nucl. Fus.*, submitted: 04/28/2016.
[8] R.J. Goldston, R. Myers, J. Schwartz, The lithium vapor box divertor, Phys. Scr. 2016 (2016) 014017.
[9] K. Tobita, et al., First wall issues related with energetic particle deposition in a tokamak fusion power reactor, Fus. Eng. Des. 65 (2003) 561–568.
[10] M. Desecures, L. El-Guebaly, F. Druyts, P. Van Iseghem, V Massaut, G. Van Oost, Study of radioactive inventory generated from W-based components in ITER and PPCS fusion designs, Fus. Eng. Des. 88 (2013) 2674–2678.
[11] P. Fiflis, A. Press, W. Xu, D. Andruczyk, D. Curreli, D.N. Ruzic, Wetting properties of liquid lithium on select fusion relevant surfaces, Fus. Eng. Des. 89 (2014) 2827–2832.
[12] P. Fiflis, Performance of the lithium metal infused trenches in the magnum PSI linear plasma simulator, Nucl. Fus. 55 (2015) 113004.
[13] S. Hammouti, et al., Elaboration of submicron structures on PEEk polymer by femtosecond laser, Appl. Surf. Sci. 327 (2015) 277–287.
[14] A.Y. Vorobyev, C. Guo, Femtosecond laser nanostructuring of metals, Opt. Express 14 (2006) 2164–2169.
[15] G. Whyman, E. Bormashenko, T. Stein, The rigorous derivation of the Young, Cassie–Baxter and Wenzel equations and the analysis of the contact angle hysteresis phenomenon, Chem. Phys. Lett. 450 (2008) 355–359.
[16] M. Szott, et al., Wetting of lithium on nanostructured surfaces for first wall components, in: IEEE 26th Symposium on Fusion Engineering (SOFE), 2015, p. 4.
[17] A. Marmur, Wetting on hydrophobic rough surfaces: to be heterogeneous or not to be? Langmuir 19 (2003) 8343–8348.
[18] W. Xu, D. Curreli, D.N. Ruzic, Computational studies of thermoelectric MHD driven liquid lithium flow in metal trenches, Fus. Eng. Des. 89 (December 12) (2014) 2868–2874 *ISSN 0920-3796*.
[19] S.I. Abdel-Khalik, Thermal-hydraulic studies in support of the Aries CS T-tube divertor design, Fusion Sci. Technol. 54 (2008) 864–877.
[20] R. Kaita, et al., Low recycling and high power density handling physics in the current drive experiment-upgrade with lithium plasma-facing components, Phys. Plasmas 14 (2007) 056111.